2016 IEEE International Symposium on Intelligent Control (ISIC)
Part of 2016 IEEE Multi-Conference on Systems and Control
September 19-22, 2016. Buenos Aires, Argentina

# Augmented Reality–enhanced Structural Inspection using Aerial Robots

Christos Papachristos and Kostas Alexis

*Abstract*— **This paper investigates the arising potential when automated path planning for aerial robotic structural inspection is combined with an Augmented Reality interface that provides live feed of stereo views fused with real–time 3D reconstruction data of the environment, while allowing seamless on–the–fly adaptation of the next robot viewpoints using intuitive head motions. The proposed solution aims to address the problem of accurate inspection and mapping of structures and environments for which a prior model exists but is not accurate, potentially outdated, or does not encode important features and semantics such as human–readable indications and other texture information. To approach the problem, the robot computes an optimized inspection path given any prior knowledge of the environment, while the human operator utilizes the live camera views and the real–time derived 3D map data to locally adjust the reference trajectory of the robot, such that it visits an updated set of viewpoints which provides the desired coverage of the real environment and sufficient focus on certain features and details. An autonomous aerial robot capable of navigation and mapping in GPS–denied environments is employed and combined with the Augmented Reality interface to experimentally demonstrate the potential of the approach in structural inspection applications.**

## I. INTRODUCTION

Robotics have demonstrated their capacity to provide rapid inspection of complex areas and environments by exploiting miniaturized sensing technologies, agile navigation, and intelligent path planning techniques. Nowadays, aerial robots of very limited cost can be equipped with a multi–modal sensing suite that may contain visible light cameras [1–7], thermal imaging [8–10] or even Light Detection and Ranging (LiDAR) devices [11] and more. At the same time, progress in robotic perception has enabled the online, real–time, 3D reconstruction of the environment [12–14], tracking of areas and targets of interest [15, 16] or even semantic scene understanding [17]. Finally, the successful combination of advanced control methodologies [18, 19] with modern path planning strategies accompanied by the real–time localization and mapping capabilities of the robot, has allowed aerial robots to navigate or even explore autonomously in possibly cluttered, challenging and previously unknown environments [4, 5, 7, 20].

At the same time, our era is characterized by groundbreaking results in the field of Augmented Reality (AR). Modern AR devices are miniaturized, low–cost systems which provide live, high–quality direct views of the real–world environment fused and augmented with computer–generated sensory input such as sound, video, graphics, GPS data and more. Market forecasts indicate that within the next few years, AR devices will become prominent among computer users and will be employed for a variety of use–cases including gaming, social interaction, virtual–tours and more.

The authors are with with the Autonomous Robots Lab of the University of Nevada, Reno, 1664 N. Virginia Street, Reno, NV 89557, USA cpapachristos@unr.edu

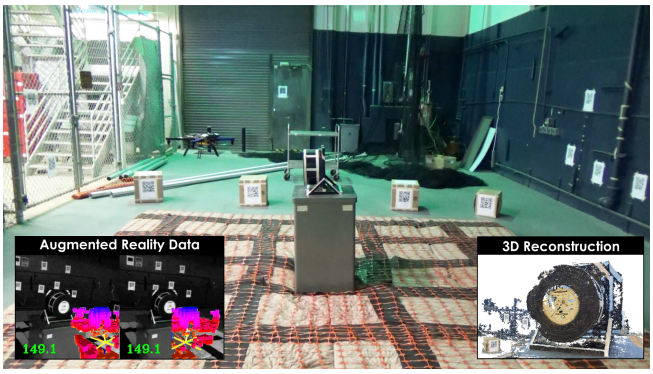


Fig. 1: Instance of an experiment for the reconstruction of a Wattmeter device. The aerial robot is following its initially computed inspection path based on a rough model of the Wattmeter, while during its operation the human operator exploits the Augmented Reality interface in order to create new viewpoints that focus more on the indication of the Wattmeter device. The whole experiment is conducted in a GPS–denied environment by only relying on the on–board visual–inertial Simultaneous Localization And Mapping system.

Within this work we investigate the arising potential when automated robotic inspection is combined with augmented reality technologies and through that the path planning capabilities and cognitive understanding of the robot is shared with the human, while at the same time human intelligence empowers the robot reactive path planning through head motion–based intuitive teleoperation. The envisioned scenario refers to industrial inspection and the utilization of aerial robots within it. In such applications, a prior model of the structure to be inspected might be available a priori, but it is typically only approximate, potentially outdated, or generally different from the real–life structure to be inspected by the aerial robot. At the same time, autonomous exploration of aerial robots is not always able to identify the information gain of areas with critical visual information (e.g. written signs, local color change). Based on this fact we want to combine methods and for automated optimized coverage path planning given the prior model of the structure, together with an AR–interface to the human inspector that provides feedback of real–time stereo views, as well as how the online 3D reconstruction is evolving. Essentially, the AR–interface enables the operator to reactively command the

978-1-5090-2051-5/16/$31.00 ©2016 IEEE

robot such that it collects the required additional views of the environment. Through such an approach, the robot can ensure the general coverage of the structure, while when a change or an area of special interest is detected, the human operator can intuitively command new viewpoints through the AR–interface and also verify their successful 3D mapping in real–time. The proposed approach and implementation are evaluated experimentally based on an autonomous aerial robot capable of navigation and 3D mapping in GPS–denied environments. Figure 1 presents an instance of this experimental study.

This paper is structured as follows: Section II defines the inspection problem as considered within this work. Section III overviews the proposed approach and how the Augmented Reality interface is fused into the robot guidance. Subsequently, Section IV provides the system technical details, while Section V describes the conducted experimental evaluation. Finally, conclusions are drawn in Section VI.

## II. PROBLEM DESCRIPTION

The problem of Augmented Reality–enhanced structural inspection path planning is, within the scope of this work, defined as the challenge to fuse automatically generated optimized inspection paths given a prior model of the inspection structure $\mathcal{S}$, with human head motion–based teleoperation commands based on the AR–interface and the streamed live feed and online 3D mapping data of the actual, real–life and potentially different than $\mathcal{S}$, structure $\mathcal{S}'$. The 3D structure to be inspected may be represented in a computationally efficient way such as a triangular mesh or a octree–based voxelgrid occupancy map (octomap) [21] and is embedded into a bounded environment that may contain obstacle regions. The problem setup is to be such that that for each triangle in the mesh, there exists an *admissible* viewpoint configuration – i.e. a viewpoint from which the triangle is visible for a specific sensor model. Then, for the given environment and with respect to the operational constraints, a path connecting all viewpoints has to be found which guarantees complete inspection of the 3D structure. Quality measures for paths are situation specific, depending on the system and mission objectives, e.g. shortest time or distance.

As a sample system we consider an aerial robot of the Micro Aerial Vehicle (MAV) class equipped with a stereo visual camera with a fixed orientation relative to the platform body frame.

## III. PROPOSED APPROACH

The proposed approach aims to develop a strategy to share the autonomous perception, locomotion and cognition capabilities of robots and human operators towards high–fidelity 3D inspection of complex structures in their environment. To address this challenge, we employ recent breakthroughs in the field of Augmented Reality and combine them with cutting–edge technologies in the field of aerial robotics. In particular, we consider aerial robotic systems capable of real–time self localization and mapping of their environment that are further empowered by path–planning algorithms which compute optimized inspection paths for any prior model of the environment that is available. The derived inspection solution corresponds to an initial path for the robot, the prior of how the inspection mission should take place if the real environment were identical to its geometrical model and each surface subset of it held equal importantance. However, as the real environment to be inspected may differ from the available model, as important information (e.g. human–readable indications or semantically–important texture) might not be encoded into its a priori known geometric model, and since it is possible that only the human operator may be able to know where to focus the inspection mission, the Augmented Reality interface aims to allow the operator to adjust the viewpoints followed by the robot. To achieve this goal efficiently, the AR–interface shares part of the robot cognition to the human by projecting synthesized stereo images that fuse the camera frames with the real–time derived 3D map of the environment. This on one hand enables the human operator to know both what the robot perceives as well as how well the environment is mapped, while on the other also allowing to derive conclusions about which part of the environment is not inspected at all or has to be further mapped and inspected in more detail. The operator can then employ head motion to intuitively guide the robot through a head motion–based teleoperation controller that adjusts the reference waypoint of the robot. Within the next sections, the employed structural inspection planner is summarized, followed by a description of the Augmented Reality interface, the cognition sharing scheme, and the control structure.

### A. Structural Inspection Planner

The proposed approach utilizes a structural inspection planner that provides an optimized full coverage solution path $\mathbf{p^I}$ (a sequence of $[x, y, z, \psi]$ configurations while roll and pitch are considered to be near zero) for the prior structure $\mathcal{S}$, the set of vehicle motion constraints as well as a sensor model for the on–board camera. Given the maximum travel speed for inspection $v_T^I$ and the maximum allowed yaw rate $\dot{\psi}_{\max}^I$, the computed path is timed at each step. Different structural inspection path planning methods may be employed, while within the framework of this work the Structural Inspection Planner (SIP) algorithm previously proposed by one of the authors [7] is employed due to its performance and the fact that is has been released as an open source package. SIP considers a triangular mesh representation of the structure $\mathcal{S}$ and computes a good full coverage path via an optimization method that alternates between two steps, namely a step that samples and computes new viewpoints such as to reduce the cost–to–travel between each viewpoint and its neighbors while maintaining full coverage, and a step that computes the optimal, collision–free connecting tour for the current iteration. The specific planner, supports both rotorcraft as well as fixed–wing aerial vehicles, and accounts for their different motion model. Furthermore, its computational cost is particularly small due to the convexification of the viewpoint computation problem and the utilization of the Lin–Kernighan–Helsgaun

(LKH) [22] solver for the tour computation step. Computational analysis is included in the relevant publication [7], while code, demo scenarios and experimental datasets are available online [23]. Alternative inspection algorithms are available in the literature, among them the works in [4, 24], also proposed by one of the authors.

### B. Augmented Reality Interface

To enable the human operator to focus only on these subsets of the structure that are not sufficiently 3D–reconstructed, either because they were not part of the prior model $\mathcal{S}$ or because they are of particular interest, the AR–interface provides a fused live view that projects both the stereo views of the camera as well as the real–time derived 3D model of the environment using the octomap-voxelgrid representation. The video is streamed over a regular Wi–Fi network with the help of the Gstreamer [25] pipeline which handles the tasks of x264 video encoding in $zero-latency$ mode, $RTP–UDP$ protocols–based streaming, and decoding on the Android (smartphone) side. Eventually the aforementioned data are projected on the smartphone–based AR–interface, with an indicative screenshot of the result depicted in Figure 2. It is noted that the 3D representation of the world–mapping is separately rendered for the left and right eye so as to maintain the human operator's immersion and stereoscoping understanding of depth. As the operator observes this fused live feed, head motion may be employed to redirect the aerial robot such that its viewpoint sequence is adapted in order to enable the accurate inspection of $\mathcal{S}'$ and its textured regions.

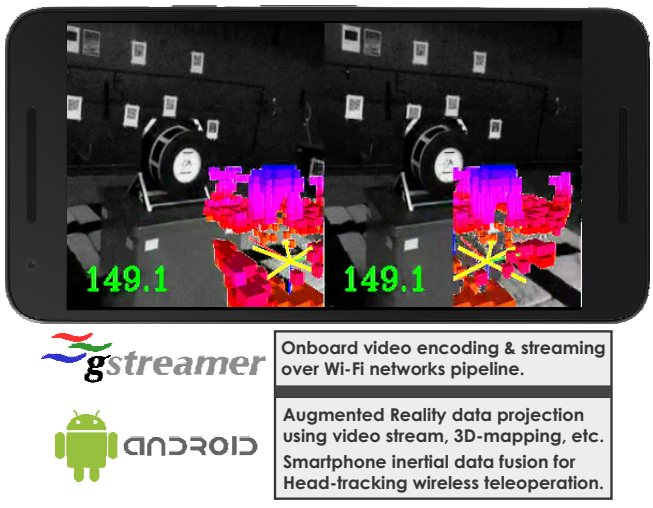


Fig. 2: Screenshot of the live feed at the Augmented Reality interface. As shown the stereo visual frames are projected fused with the real–time derived volumetric 3D reconstruction of the environment. For efficient data transfer over the Wi–Fi channel, the feed is encoded and streamed to the smartphone device with the help of the Gstreamer pipeline.

To implement the aforementioned concept, the custom–developed smartphone software apart from video decoding based on an Android NDK–driven implementation of the Gstreamer libraries also handles the the tasks of head motion tracking and teleoperation control. Head–tracking is achieved through the fusion of the inertial and orientation measurement unit data acquired from the Android Sensors API [26] of the smartphone device, in a custom-made Extended Kalman Filter (EKF) structure. Given that head motion estimation is robustly operating, the teleoperation controller can function to adjust the waypoints followed by the robot between two sequential viewpoints of the initial inspection solution $\mathbf{p^I}$. Among two subsequent viewpoints $\mathbf{p^I}_i$ and $\mathbf{p^I}_j$, rolling & pitching head motions and orientation change are mapped to lateral & vertical translations of the robot reference, as well as change of its heading angle. More specifically, let $\mathbf{n}_{\mathbf{x}_r \rightarrow \mathbf{p^I}_j}$ denote the normal vector between the current position of the robot $\mathbf{x}_r$ towards its next originally-computed waypoint $\mathbf{p^I}_j$. Then, the adjusted intermediate waypoint takes the form:

$$p' = \min(|\mathbf{x}_r, \mathbf{p^I}_j|, d_{\max})\mathbf{n}' \ , \tag{1}$$

where $d_{\max}$ is a tunable maximum waypoint distance value and $\mathbf{n}'$ represents the new normal vector that points towards the updated waypoint. The latter takes the form $\mathbf{n}' = \mathbf{n}_{\mathbf{x}_r \rightarrow \mathbf{p^I}_j} + \mathbf{R}_b^V(0, \Delta y, \Delta z)$, where $\mathbf{R}_b^V$ is the body to inertial frame rotation matrix and $\Delta y, \Delta z$ are the lateral translations directed by the user based on two gains $k_l, k_v$ that map the rolling and pitching motions of the head to lateral and vertical distances correspondingly.

## IV. SYSTEM DESCRIPTION

A custom–built autonomous aerial robot design is employed for the research studies conducted within this paper. The system is of the quadrotor class, has a mass of $m = 2.2$kg and integrates advanced processing and perception systems to enable its autonomous operation in GPS–denied environments.

More specifically, the robot is primarily controlled through a low– and top–level processing structure with the first being responsible for the attitude control functionalities and the second consisting of a high–level processing unit as well as an intermediate processor that together handle the self localization and mapping process, the position control of the system, and the communication with the AR–interface, while also providing redundancy options. The low–level attitude control system is designed around the open–source Pixhawk autopilot [27] but runs a custom software with a Proportional-Integral-Derivative-second Derivative control scheme for the roll, pitch and yaw dynamics of the vehicle and a loop frequency of $400$Hz. The high–level processor is based on an Intel i7–based Next Unit of Computing (NUC) and interfaces a stereo visual–inertial system consisting of a ZED Stereo Camera (baseline of $0.12$m, effective Field of View of $60, 60$ degrees around the horizontal and vertical axes) and a CH–Robotics UM7 Inertial Measurement Unit which are then software synchronized. Based on the synchronized visual–inertial data, the system runs the Open Keyframe–based Visual–Inertial Simultaneous Localization

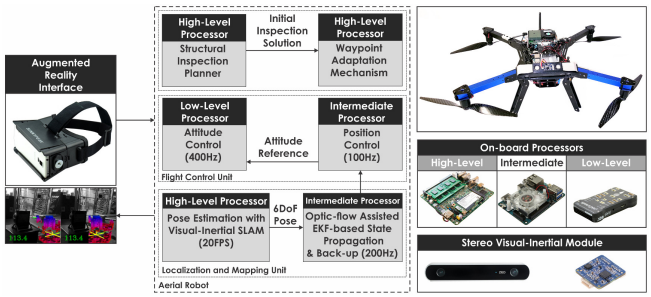


Fig. 3: Overview of the main components functionalities on–board the aerial robot and their interconnection with the AR–interface. The AR–interface receives a rendered image that depicts the stereo camera frames annotated with the real–time derived 3D reconstruction of the environment.

and Mapping framework [28] which provides the pose estimate of the robot at 20Hz, while also deriving a sparse map of the environment. This sparse map of the environment is then densified and a volumetric, octomap–based representation of the it is computed and used for collision–free navigation within the environment using RRT$^\star$ as the planning module. Furthermore, the stereo visual frames and the dense map of the environment are combined, rendered in a single stereo–view projection and sent to the AR–interface through a Wi–Fi channel. In addition, the derived pose estimate of the aerial robot is then fed to an ODROID XU4–based intermediate processing system which further interfaces a nadir–facing PSEye camera system with an Optical Flow estimation scheme [29] that operates at 100Hz. Furthermore, the intermediate processing system fuses the 6 Degrees of Freedom (DoF) pose estimate coming from the visual–inertial navigation system of the high–level processor with the optic flow–based velocity estimate and then delivers a robustified full pose estimate at 100Hz through an EKF structure running multiple prediction steps per full–pose correction. Based on this pose estimate, the intermediate processing unit then runs the position control loop (100Hz) of the system, relying on a Proportional–Integral–Derivative structure, and feeds the attitude and thrust references to the low–level unit. Through such an architecture, the intermediate processor also acts as redundancy unit and is able to ensure stable hovering and landing of the system in case of failure of the, necessarily more complex, visual–inertial localization scheme running on the high–level processing unit. The overall system architecture is presented in Figure 3.

The AR–interface is deployed on a Samsung S4 Android smartphone and a Sunnypeak Virtual–Reality headset. A dedicated application is developed and performs state estimation, teleoperation control and projects the fused, rendered stereo view together with the real–time derived 3D reconstruction of the environment. Using this Augmented Reality feedback, the human operator can then decide on where should the robot be redirected in order to perceive parts of the real structure $\mathcal{S}'$ that were not present at the prior model $\mathcal{S}$ or focus in areas that are of particular interest (e.g. the indication of a measurement device). Feedback to the robot is provided by tracking the head motion through the fusion of the inertial sensor suite available on the smartphone device (accelerometers & magnetometers and potentially gyroscopes). The previously mentioned EKF implemented within the Android application is then employed to estimate the head roll, pitch and yaw motions which are subsequently mapped to lateral & vertical and orientation deviations of the robot reference waypoint. These commands are then forwarded via the same Wi–Fi link to the aerial robot, and are handled as waypoint–modification references based on (1) by its onboard trajectory–following scheme. Special indications which correspond to these head–tracking based inputs are visually overlaid onto the finally projected screen, offering real–time visual feedback to the human-operator regarding the commands that they impose onto the aerial robot. Figure 4 illustrates these concepts more specifically, and overviews the integration of the AR–interface to the overall robotic system.

It is eventually highlighted that the octomap–based 3D reconstruction of the environment rendering is a Third–Person perspective viewpoint, which acts complementarily to the First–Person perspective offered by the direct onboard stereo video stream, in the sense that it maintains a larger subset of the mapped environment structures within the human operator's AR–based field of view.

This integrated Augmented Reality–enhanced robotic system is employed to conduct the evaluation study presented within this paper. Among its several capabilities, the capacity for autonomous localization and mapping in GPS–denied environments, the real–time dense reconstruction, as well as the on–board rendering of the AR–interface data correspond to the key functionalities that enable the contributions of this paper.

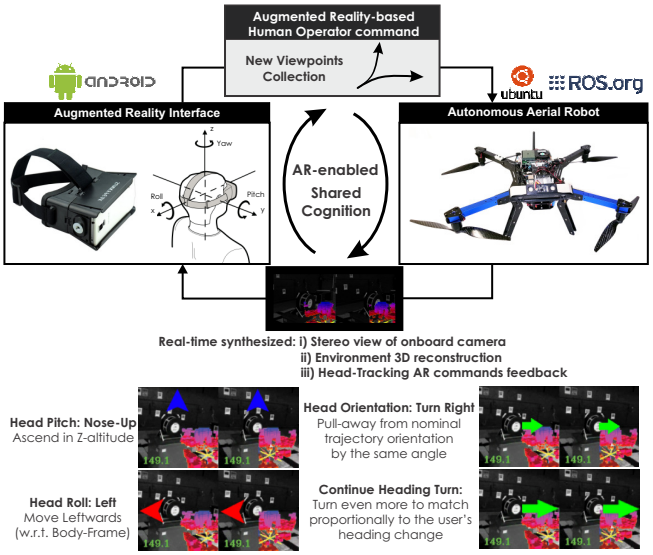


Fig. 4: Overview of the functionality of the Augmented Reality interface. The user uses the live feed of synthesized data consisting of live stereo view and real–time derived 3D reconstruction of the environment in order to command updated reference viewpoints for the aerial robot.

## V. EXPERIMENTAL STUDIES

To demonstrate the potential of the proposed approach, an experimental study inspired by industrial inspection applications is conducted. More specifically, an analog Wattmeter acts as the structure to be inspected. For this device, a prior 3D model is considered to be available (from a rough CAD design) but on one hand it is less accurate (consisting only of 173 mesh faces), and on the other it does not contain information regarding which part of it is more important. In real–life however, it is expected that the human operator would have interest to focus more on the indication of the Wattmeter device while relying on the robot autonomous navigation for the rest of the structure. As demonstrated, this behavior is seamlessly provided through the proposed Augmented Reality–enhanced aerial robotic inspection solution.

The experiment takes place in the Autonomous Robots Arena facilities of the University of Nevada, Reno and relies on the previously described custom–built autonomous aerial robot that is capable of GPS–denied flight due to its visual–inertial navigation solution. No support from the motion capture system is provided. The structural inspection planner is utilized to derive the initial inspection path, while during the operation a human is using the head–mounted AR–interface to keep track of the camera data collected by the robot as well as of the progress of the online 3D reconstruction. Within the subset of the experiment that the robot is facing towards the Wattmeter indication, the human is commanding additional viewpoints through appropriate head motion. Figure 5 presents the derived experimental results, while a video of the experiment –annotated with the Augmented Reality data and user commands– is provided online at `http://www.kostasalexis.com/augmented-reality.html`.

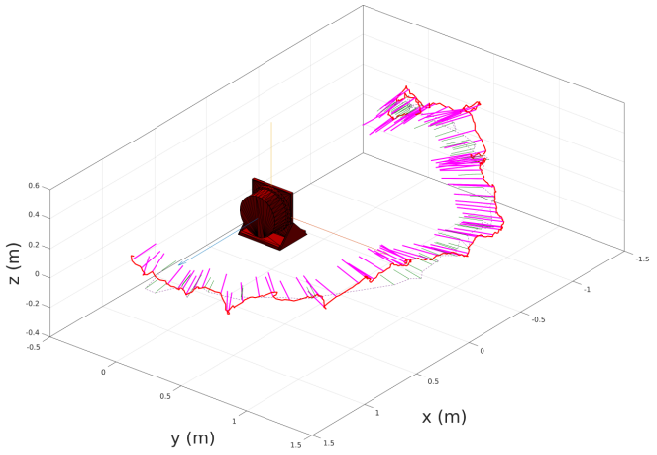


Fig. 5: Collective inspection path based on the initial inspection path computed by the robot as well as the human operator commands provided based on the data of the AR–interface and the tracked head motion which is then mapped to lateral, vertical and yaw deviations of the reference trajectory of the robot.

To present the operation of the AR–interface, Figure 6 shows the timeseries values for the experimental sequence. More specifically, the top subfigure illustrates the translational trajectory reference signals and the actually followed path by the UAV, the middle one shows the respective values for the UAV's orientation, and the bottom one indicated the Augmented Reality commands overlaid the the human operator–inspector.

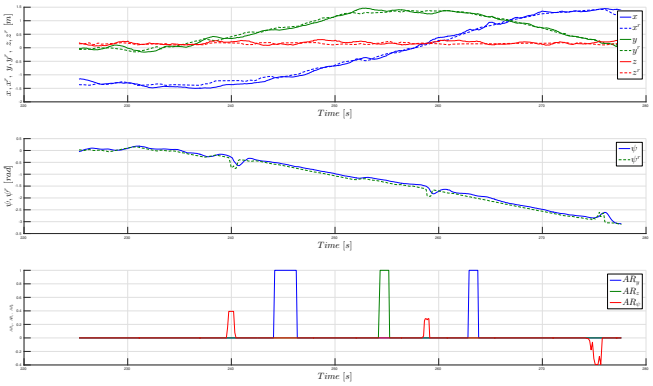


Fig. 6: Trajectory reference commands and actual trajectory followed by the UAV. Bottom sub-figure shows the overlaid Lateral ($AR_y$), Vertical ($AR_z$), and Yaw-deviation ($AR_\psi$) Augmented Reality commands respectively.

In addition to these results, the reconstructed 3D model of the Wattmeter is shown in Figure 7. As shown, a high–fidelity reconstruction solution is achieved primarily on the area of the Wattmeter's analog indicator dials, where the user primarily instructed new viewpoints to be collected.

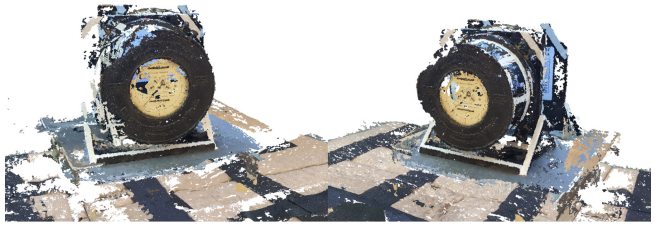

Fig. 7: Dense reconstruction of the 3D model of the Wattmeter device based on the on–board derived camera data and simultaneous localization and mapping pipeline. An additional densification step has taken place offline to improve the visual quality of the derived 3D model. Close inspection reveals that even the analog indicator is visible on the model.

## VI. CONCLUSIONS

An approach to combine autonomous robotic inspection with Augmented Reality–enabled human teleoperation is proposed and aims to address the problem of robotic inspection of structures and environments for which prior knowledge exists but it is relatively outdated or does not encode areas of interest and other important features. The method employs a previously proposed structural inspection planner which derives the initial inspection trajectory given any prior knowledge of the environment. Live feed of the stereo camera frames combined with the real–time 3D reconstruction of the environment is provided to the human operator via the Augmented Reality interface. Once an area that needs special attention, or is not 3D–mapped and

reconstructed at sufficient levels of fidelity by the initial robot trajectory is detected, then head motion may be employed to adjust the path of the robot and collect the required viewpoints. The overall framework is demonstrated with the use of an aerial robot capable of GPS–denied navigation and online mapping of its environment.

## REFERENCES


[1] M. Burri, J. Nikolic, C. Hurzeler, G. Caprari, and R. Siegwart, "Aerial service robots for visual inspection of thermal power plant boiler systems," in *Applied Robotics for the Power Industry, 2012 2nd International Conference on*, 2012.

[2] J. Nikolic, J. Rehder, M. Burri, P. Gohl, S. Leutenegger, P. T. Furgale, and R. Y. Siegwart, "A Synchronized Visual-Inertial Sensor System with FPGA Pre-Processing for Accurate Real-Time SLAM," in *IEEE International Conference on Robotics and Automation (ICRA)*, 2014.

[3] C. Papachristos, K. Alexis, L. R. G. Carrillo, and A. Tzes, "Distributed infrastructure inspection path planning for aerial robotics subject to time constraints," in *2016 International Conference on Unmanned Aircraft Systems (ICUAS)*. IEEE, 2016, pp. 406–412.

[4] A. Bircher, M. Kamel, K. Alexis, H. Oleynikova and R. Siegwart, "Receding horizon "next-best-view" planner for 3d exploration," in *IEEE International Conference on Robotics and Automation (ICRA)*, May 2016. [Online]. Available: https://github.com/ethz-asl/nbvplanner

[5] A. Bircher, M. Kamel, K. Alexis, M. Burri, P. Oettershagen, S. Omari, T. Mantel and R. Siegwart, "Three-dimensional coverage path planning via viewpoint resampling and tour optimization for aerial robots," *Autonomous Robots*, pp. 1–25, 2015.

[6] L. Zikou, C. Papachristos, K. Alexis, and A. Tzes, "Inspection operations using an aerial robot powered-over-tether by a ground vehicle," in *Advances in Visual Computing*, ser. Lecture Notes in Computer Science. Springer International Publishing, 2015, vol. 9474, pp. 455–465. [Online]. Available: http://dx.doi.org/10.1007/978-3-319-27857-5_41

[7] A. Bircher, K. Alexis, M. Burri, P. Oettershagen, S. Omari, T. Mantel and R. Siegwart, "Structural inspection path planning via iterative viewpoint resampling with application to aerial robotics," in *IEEE International Conference on Robotics and Automation (ICRA)*, May 2015, pp. 6423–6430. [Online]. Available: https://github.com/ethz-asl/StructuralInspectionPlanner

[8] P. Oettershagen, T. Stastny, T. Mantel, A. Melzer, K. Rudin, G. Agamennoni, K. Alexis, and R. Siegwart, "Long-endurance sensing and mapping using a hand-launchable solar-powered uav," June 2015.

[9] Rudol, P. and Doherty, P., "Human body detection and geolocalization for uav search and rescue missions using color and thermal imagery," in *Aerospace Conference, 2008 IEEE*, 2008, pp. 1–8.

[10] P. Rudol and P. Doherty, "Human body detection and localization for uav search and rescue missions using color and thermal imagery," in *Aerospace Conference, 2008 IEEE*. IEEE, 2008, pp. 1–8.

[11] J. Zhang and S. Singh, "Loam: Lidar odometry and mapping in real-time," in *Robotics: Science and Systems Conference (RSS)*, 2014, pp. 109–111.

[12] S. Omari, P. Gohl, M. Burri, M. Achtelik, and R. Siegwart, "Visual industrial inspection using aerial robots," in *Applied Robotics for the Power Industry (CARPI), 2014 3rd International Conference on*. IEEE, 2014, pp. 1–5.

[13] S. Lynen, M. W. Achtelik, S. Weiss, M. Chli, and R. Siegwart, "A robust and modular multi-sensor fusion approach applied to mav navigation," in *Intelligent Robots and Systems (IROS), 2013 IEEE/RSJ International Conference on*. IEEE, 2013, pp. 3923–3929.

[14] S. Omari, M. Bloesch, P. Gohl, and R. Siegwart, "Dense visual-inertial navigation system for mobile robots," in *Robotics and Automation (ICRA), 2015 IEEE International Conference on*. IEEE, 2015, pp. 2634–2640.

[15] C. Papachristos, D. Tzoumanikas, and A. Tzes, "Aerial robotic tracking of a generalized mobile target employing visual and spatio-temporal dynamic subject perception," in *Intelligent Robots and Systems (IROS), 2011 IEEE-RSJ International Conference on*, Sept-Oct 2015, pp. 4319–4324.

[16] C. Papachristos, D. Tzoumanikas, K. Alexis, and A. Tzes, "Autonomous robotic aerial tracking, avoidance, and seeking of a mobile human subject," in *Advances in Visual Computing*, ser. Lecture Notes in Computer Science. Springer International Publishing, 2015, vol. 9474, pp. 444–454. [Online]. Available: http://dx.doi.org/10.1007/978-3-319-27857-5_40

[17] J. Fernandez Galarreta, N. Kerle, and M. Gerke, "Uav-based urban structural damage assessment using object-based image analysis and semantic reasoning," *Natural Hazards and Earth System Science*, vol. 15, no. 6, pp. 1087–1101, 2015.

[18] K. Alexis, C. Papachristos, R. Siegwart, and A. Tzes, "Robust model predictive flight control of unmanned rotorcrafts," *Journal of Intelligent & Robotic Systems*, pp. 1–27, 2015. [Online]. Available: http://dx.doi.org/10.1007/s10846-015-0238-7

[19] C. Papachristos, K. Alexis, and A. Tzes, "Dual–authority thrust–vectoring of a tri–tiltrotor employing model predictive control," *Journal of Intelligent & Robotic Systems*, pp. 1–34, 2015. [Online]. Available: http://dx.doi.org/10.1007/s10846-015-0231-1

[20] A. Bircher, K. Alexis, U. Schwesinger, S. Omari, M. Burri, and R. Siegwart, "An incremental sampling-based approach to inspection planning: The rapidly-exploring random tree of trees," 2015.

[21] A. Hornung, K. M. Wurm, M. Bennewitz, C. Stachniss, and W. Burgard, "OctoMap: An efficient probabilistic 3D mapping framework based on octrees," *Autonomous Robots*, 2013.

[22] K. Helsgaun, "An effective implementation of the lin–kernighan traveling salesman heuristic," *European Journal of Operational Research*, vol. 126, no. 1, pp. 106–130, 2000.

[23] Andreas Bircher, and Kostas Alexis, "Structural Inspection Planner Code Release." [Online]. Available: https://github.com/ethz-asl/StructuralInspectionPlanner

[24] K. Alexis, C. Papachristos, R. Siegwart, and A. Tzes, "Uniform coverage structural inspection path-planning for micro aerial vehicles," September 2015.

[25] "Open source multimedia framework," Tech. Rep. [Online]. Available: https://gstreamer.freedesktop.org/

[26] "Android sensors api," Tech. Rep. [Online]. Available: https://developer.android.com/guide/topics/sensors/sensors_overview.html

[27] PIXHAWK Autopilot, "http://px4.io/."

[28] S. Leutenegger, S. Lynen, M. Bosse, R. Siegwart, and P. Furgale, "Keyframe-based visual–inertial odometry using nonlinear optimization," *The International Journal of Robotics Research*, vol. 34, no. 3, pp. 314–334, 2015.

[29] C. Papachristos, K. Alexis and A. Tzes, "Model predictive hovering–translation control of an unmanned tri–tiltrotor," in *2013 International Conference on Robotics and Automation*, Karlsruhe, Germany, 2013, pp. 5405–5412.